Ocean Systems Engineering, *Vol. 13, No. 2 (2023) 97-121*
https://doi.org/10.12989/ose.2023.13.2.097

Effects of geometrical parameters on the degree of bending in two-planar tubular DYT-joints of offshore jacket structures

Hamid Ahmadi*[1,2,3] and Mahdi Ghorbani[2]

[1]*Centre for Future Materials, University of Southern Queensland, QLD 4350, Australia*
[2]*Faculty of Civil Engineering, University of Tabriz, Tabriz 5166616471, Iran*
[3]*Center of Excellence in Hydroinformatics, University of Tabriz, Tabriz 5166616471, Iran*

(Received January 10, 2023, Revised March 26, 2023, Accepted April 6, 2023)

Abstract. Through-the-thickness stress distribution in a tubular member has a profound effect on the fatigue behavior of tubular joints commonly found in steel offshore structures. This stress distribution can be characterized by the degree of bending (DoB). Although multi-planar joints are an intrinsic feature of offshore tubular structures and the multi-planarity usually has a considerable effect on the DoB values at the brace-to-chord intersection, few investigations have been reported on the DoB in multi-planar joints due to the complexity of the problem and high cost involved. In the present research, data extracted from the stress analysis of 243 finite element (FE) models, verified based on available parametric equations, was used to study the effects of geometrical parameters on the DoB values in two-planar tubular DYT-joints. Parametric FE study was followed by a set of nonlinear regression analyses to develop six new DoB parametric equations for the fatigue analysis and design of axially loaded two-planar DYT-joints.

Keywords: degree of bending (DoB); fatigue; offshore jacket structure; two-planar tubular DYT-joint

1. Introduction

Jacket-type platform is the most common type of fixed offshore structures employed for the production of oil and gas from the hydrocarbon reservoirs below the seabed. The primary structural part of an offshore jacket-type platform, i.e., the jacket substructure (Fig. 1(a)), is fabricated from tubular members by welding one end of the branch members, i.e., braces, to the undisturbed surface of the main member, i.e., chord, resulting in what is known as a tubular joint (Fig. 1(b)). As a result of the formation and propagation of cracks due to wave induced cyclic loads, tubular joints are susceptible to fatigue-induced damage during their service life. Fatigue life, reliability, and design challenges of steel offshore structures have been discussed by Ju (2022), Wang *et al*. (2022), and Sunday and Brennan (2021), among others.

The stress-life (S-N) approach, adopted by major offshore design codes and standards such as API RP 2A (2007), DNV OS C201 (2008), and DNV RP C203 (2005), is widely used to estimate the fatigue life of a tubular joint and it is based on the hot-spot stress (HSS) calculation. Hot-spot stresses in multi-planar tubular joints have been extensively studied by Bao *et al*. (2020, 2022a, b,

*Corresponding author, E-mail: h-ahmadi@tabrizu.ac.ir; hamid.ahmadi@usq.edu.au

http://www.techno-press.org/?journal=ose&subpage=7 ISSN: 2093-6702 (Print), 2093-677X (Online)

2023). However, studies on a large number of fatigue test results have shown that tubular joints of different geometry or loading type but with similar HSS values often exhibit significantly different numbers of cycles to failure (Connolly 1986). Such differences are thought to be attributable to changes in crack growth rate that depends on the through-the-thickness stress distribution which can be characterized by the degree of bending (DoB) defined as the ratio of bending stress to total stress. Fig. 2 depicts the typical stress distribution through the chord wall of a tubular joint. Through-the-thickness stress field is a combination of the linear stress due to the chord wall bending and the nonlinear stress concentration at the weld toe due to the section change at the intersection. The nonlinear stress distribution around the weld toe is dependent on the weld geometry and is difficult to predict during the design stage. Since for a deep crack, the weld-toe stress concentration has a relatively little effect on the through-the-thickness stress field (Chang and Dover 1999b), the stress distribution across the wall thickness is usually assumed to be a linear combination of membrane and bending stresses. Hence, the DoB can be expressed as

$$\mathrm{DoB} = \frac{\sigma_B}{\sigma_T} = \frac{\sigma_B}{\sigma_B + \sigma_M} \tag{1}$$

where σ_T is the total stress; and σ_B and σ_M are the bending and membrane stress components, respectively.

Although the weld-toe stress concentration has a relatively little effect on the through-the-thickness stress field, it still has a considerable effect on the stress distribution along the weld toe. Hence, it should be noted that since the weld-toe stress concentration directly affects the rate of the fatigue crack growth, its effect should be considered in the formulation of the stress intensity factor (SIF) as indicated in Eq. (23) of Sect. 6. In fact, Eq. (23) shows that the effects of both linear and nonlinear parts of the stress distribution are considered in the calculation of the fatigue crack growth rate by implementing both the DoB and the stress concentration factor (SCF) in the formulation of the SIF.

Previous studies have shown that the standard stress-life approach may be unconservative for the joints with low DoB. For example, results of the tubular joint fatigue tests conducted by Eide *et al.* (1993) confirmed the detrimental effect of low DoB on fatigue life. It was found that the experimentally measured fatigue life is significantly shorter compared to the prediction using the S-N curve method. According to Chang and Dover (1999b), finite element analyses of tubular joints have shown that typical DoB values are in the range of 0.8–0.9 for the joints used to derive the S-N curves. Smaller values can be considered as low DoB. For the double T specimens studied by Eide *et al*. (1993), a DoB of 0.69 was measured. Hence, the current standard HSS-based S-N approach can be modified to include the effect of DoB in order to obtain more accurate fatigue life prediction. The other shortcoming of the S-N approach is that this method gives only the total life and cannot be used to predict the fatigue crack growth and the remaining life of cracked joints. For the fatigue analysis of cracked joints, fracture mechanics (FM) should be used. The accurate determination of the SIF is the key for FM calculations. Owing to the complexities introduced by the structural geometry and the nature of the local stress fields, it is impossible to calculate the SIFs analytically. This problem is often tackled by using the simplified models, such as the flat plate solution and methods based on the T-Butt weight function with an appropriate load shedding model. In order to use these simplified SIF models to calculate the remaining fatigue life of tubular joints, the information is required again on the distribution of through-the-thickness stress acting on the anticipated crack path, which can be characterized by the DoB. Thus, the DoB is an important input

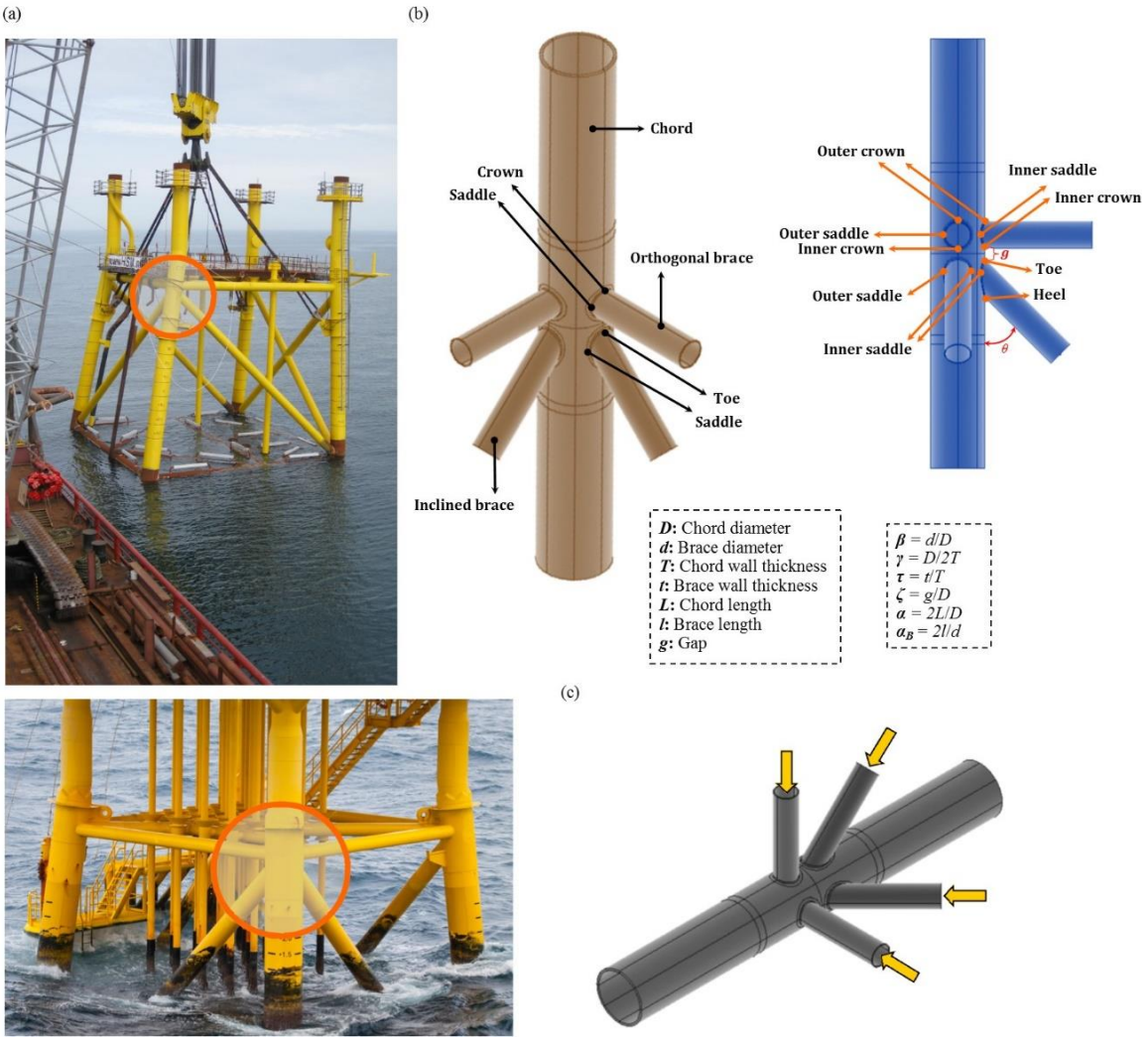

Fig. 1 (a) Two-planar tubular DYT-joints in offshore jacket structures, (b) Geometrical notation for a two-planar DYT-joint and (c) Studied axial loading condition

parameter for the calculation of fatigue crack growth in tubular welded joints. Details of the DoB application to improve the accuracy of fatigue life estimations using the S-N and FM approaches are discussed in Sect. 6.

Under any specific loading condition, the DoB value along the weld toe of a tubular joint is mainly determined by the joint geometry. To study the behavior of a tubular joint and to easily relate this behavior to the geometrical characteristics of the joint, a set of dimensionless geometrical parameters has been defined. Fig. 1(b) depicts a two-planar tubular DYT-joint with the geometrical parameters τ, γ, β, θ, ζ, α, and α_B for chord and brace diameters D and d, their corresponding wall thicknesses T and t, and respective lengths L and l. Critical positions along the weld toe of the brace-to-chord intersection for the calculation of the DoB values in a tubular DYT-joint, i.e., inner saddle, outer saddle, inner crown, outer crown, toe, and heel have been shown in Fig. 1(b).

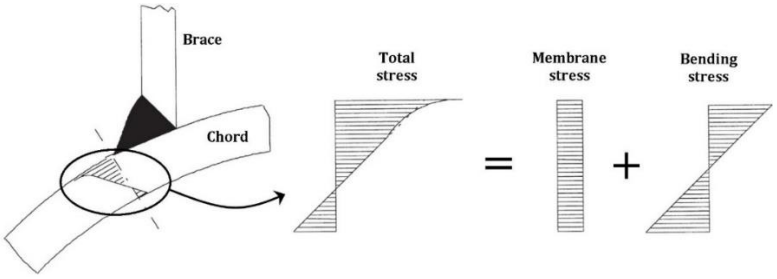

Fig. 2 Through-the-thickness stress distribution in the chord member of a tubular joint

Since early 1990s, a number of research works has been devoted to the study of the DoB in simple tubular connections such as X- and K-joints. As a result, a set of parametric design formulas in terms of the joint's geometrical parameters have been proposed providing the DoB values at certain positions adjacent to the weld for several loading conditions. However, for tubular joints having more complex geometry such as multi-planar connections which cover the majority of practical applications, much fewer investigations have been reported.

In the present paper, results of a numerical investigation on the DoB values in two-planar tubular DYT-joints are presented and discussed. In this research program, a set of parametric finite element (FE) stress analyses was carried out on 243 two-planar tubular DYT-joint models subjected to axial loading (Fig. 1(c)). In-plane bending (IPB) and out-of-plane bending (OPB) moment loadings are not covered in the present research. Analysis results were used to present general remarks on the effects of geometrical parameters including τ (brace-to-chord thickness ratio), γ (chord wall slenderness ratio), β (brace-to-chord diameter ratio), θ (brace inclination angle), and α (chord length-to-radius ratio) on the DoB values at the inner saddle, outer saddle, inner crown, outer crown, and toe positions. Based on the results of DYT-joint FE models, verified using available parametric equations, a DoB database was prepared. Then, a new set of DoB parametric equations was established, based on nonlinear regression analyses, for the fatigue analysis and design of two-planar tubular DYT-joints subjected to axial loading. The reliability of proposed equations was evaluated according to the acceptance criteria recommended by the UK Department of Energy (1983).

2. Literature review

Morgan and Lee (1998b) derived mean and design equations for DoB values at critical positions in axially loaded tubular K-joints from a previously established FE database of 254 joints. Design equations met all the acceptance criteria recommended by the UK DoE (1983). Chang and Dover (1999b) carried out a series of systematic thin-shell FE analyses for 330 tubular X- and DT-joints typically found in offshore structures under six different types of loading. Based on the results of nearly 2000 FE analyses, a set of parametric equations was developed to calculate the DoB at critical positions.

Lee and Bowness (2002) proposed an engineering methodology for estimating SIF solutions for semi-elliptical weld-toe cracks in tubular joints. The methodology uses the T-butt solutions proposed previously by the authors in conjunction with the SCFs and the DoB values in uncracked tubular joints. Shen and Choo (2012) determined the SIFs for a grouted tubular joint. They found that the fatigue strength of a grouted joint may be lower than that of as-welded joint, because when

normalized with the HSS, the shape factor of grouted joint is higher than that of original as-welded joint due to the reduction in the DoB caused by the presence of in-filled grout in the chord. For grouted tubular joints, it is essential to consider the effect of the DoB in practical fatigue assessment using HSS approach.

Ahmadi *et al*. (2015) performed a set of parametric stress analyses on 81 K-joint FE models subjected to two different types of IPB moment loading. Analysis results were used to present general remarks on the effect of geometrical parameters on the DoB values at the toe and heel positions; and a new set of DoB parametric equations was developed. Ahmadi and Asoodeh (2016) analyzed 81 K-joint FE models subjected to two types of OPB moment loading. Results were used to study the geometrical effects on the DoB at the saddle position; and two new DoB design formulas were proposed.

Ahmadi and Amini Niaki (2019) studied the degree of bending in two-planar tubular DT-joints under axial and bending loads. They developed a set of parametric equations to predict the DoB values at the saddle and crown positions. Data extracted from 648 FE analyses carried out on 81 tubular KT-joint models was used by Ahmadi and Zavvar (2020) to study the effects of geometrical parameters on the DoB values in KT-joints subjected to eight different types of axial, IPB, and OPB loadings. Generated FE models were validated using experimental data, previous FE results, and available parametric equations. Geometrically parametric investigation was followed by a set of nonlinear regression analyses to develop 21 parametric design formulas for the calculation of the DoB in tubular KT-joints under the axial, IPB, and OPB loadings.

Ahmadi *et al*. (2020) developed a set of fatigue design equations for the calculation of DoB values in multi-planar tubular XT-joints of offshore jacket-type platforms subjected to axial loading. Ahmadi and Alizadeh Atalo (2021) investigated the effect of geometrical parameters on the degree of bending in multi-planar tubular KK-joints of the jacket substructure in an offshore wind turbine. Based on the above discussion, it can be concluded that despite the comprehensive research carried out on the study of the SCF, SIF, local joint flexibility (LJF), and strength of tubular joints (e.g., Efthymiou (1988), Hellier *et al*. (1990), Morgan and Lee (1998a), Chang and Dover (1999a), Shao (2007), Shao *et al*. (2009), Nassiraei and Rezadoost (2020, 2021a-e, 2022a-c), and Ahmadi and Imani (2022) for the SCF; Shao and Lie (2005) and Shao (2006) for the SIF; Asgarian *et al.* (2014) for the LJF; and Prashob *et al*. (2018) for the strength, among many others), the research works on the DoB in tubular joints are scarce and the studied joint types are limited to simple connections. Moreover, it is evident that in spite of frequent application of DYT-joints in the design of offshore jacket structures, the DoB in such joints has not been studied so far and no parametric equation is currently available for the DoB calculation in two-planar tubular DYT-joints.

3. FE modeling and analysis of two-planar tubular DYT-joints for the DoB calculation

FE-based software package ANSYS Ver. 18 was used in the present research for the modeling and analysis of two-planar tubular DYT-joints subjected to axial loading in order to extract the DoB values for the parametric study and formulation. This section presents the details of FE modeling and analysis.

3.1 Simulation of the weld profile

Accurate modeling of the weld profile is one of the important factors affecting the accuracy of

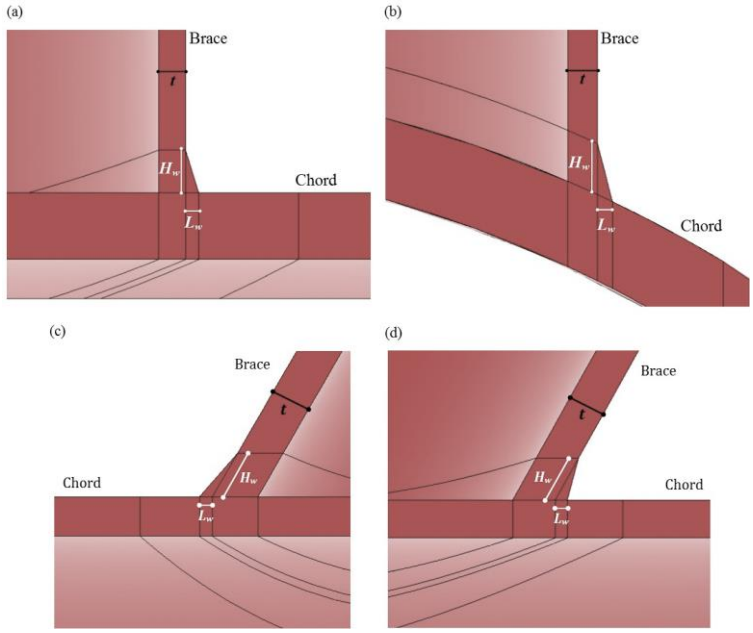

Fig. 3 Weld dimensions: (a) Crown position, (a) Saddle position, (c) Toe position and (d) Heel position

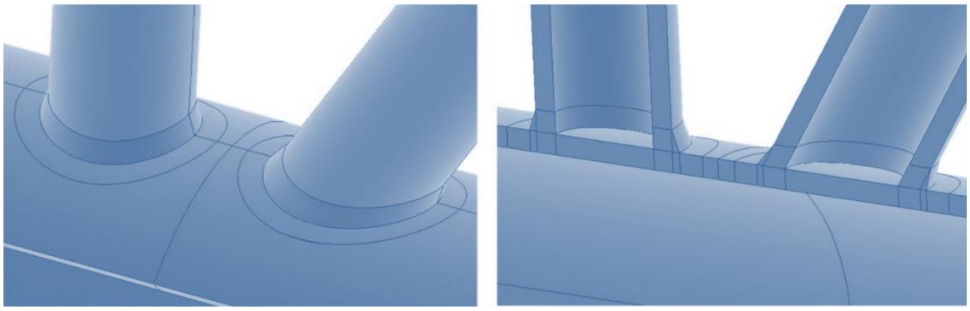

Fig. 4 Weld profile generated for a sample joint model (β = 0.3, γ = 12, τ = 1.0, θ = 60˚, α = 16)

the DoB results. In the present research, the welding size along the brace-to-chord intersection satisfies the AWS D 1.1 (2002) specifications. The weld sizes at the crown, saddle, toe, and heel positions can be determined as follows

$$H_w(\text{mm}) = 0.85t(\text{mm}) + 4.24$$
$$L_w = \frac{t}{2}\left[\frac{135^\circ - \psi\ (\text{deg.})}{45^\circ}\right] \tag{2}$$
$$\psi = \begin{cases} 90^\circ & \text{Crown} \\ 180^\circ - \cos^{-1}\beta\ (\text{deg.}) & \text{Saddle} \\ 180^\circ - \theta\ (\text{deg.}) & \text{Toe} \\ \theta\ (\text{deg.}) & \text{Heel} \end{cases}$$

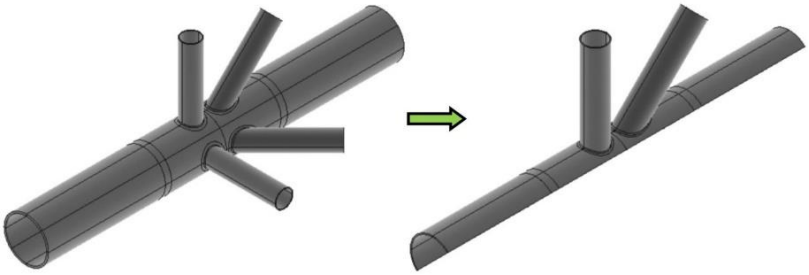

Fig. 5 One half of the entire two-planar tubular DYT-joint required to be modeled under studied axial loading condition

The parameters used in Eq. (2) are defined in Fig. 3. As an example, the weld profile generated for a sample joint model (β = 0.3, γ = 12, τ = 1.0, θ = 60°, α = 16) is shown in Fig. 4. For details of the weld profile modeling according to AWS D 1.1 (2002) specifications, the reader is referred to Lie *et al*. (2001).

3.2 Load application and boundary conditions

As shown in Fig. 1(c), applied loading condition was a combination of four compressive forces exerted axially at the end of the four brace members.

In offshore structures, the chord end fixity conditions of tubular joints may range from almost fixed to almost pinned with generally being closer to almost fixed (Efthymiou 1988). In practice, the value of the parameter α in over 60% of tubular joints is in excess of 20 and is bigger than 40 in 35% of the joints (Smedley and Fisher 1991). Changing the end restraint from fixed to pinned results in a maximum increase of 15% in the SCF at the crown position for joints with α = 6, and this increase reduces to only 8% for α = 8 (Morgan and Lee 1998b). In the view of the fact that the effect of chord end restraints is only significant for joints with α < 8 and high β and γ values, which do not commonly occur in practice, both chord ends were assumed to be fixed, with the corresponding nodes restrained.

Due to the symmetry in geometry and loading of the joint, only ½ of the entire two-planar tubular DYT-joint is required to be modeled in order to reduce the computational time (Fig. 5). Appropriate symmetric boundary conditions were defined for the nodes located on the symmetry planes.

3.3 Mesh generation

In the present study, ANSYS element SOLID95 was used to model the chord, braces, and weld profiles. This element type has compatible displacements and is well-suited to model curved boundaries. It is defined by 20 nodes having three degrees of freedom per node and may have any spatial orientation. Using this type of 3-D brick elements, the weld profile can be modeled as a sharp notch. This method will produce more accurate and detailed stress distribution near the intersection in comparison with a shell analysis.

To guarantee the mesh quality, a sub-zone mesh generation scheme was used during the FE modeling. The entire structure was divided to several zones according to computational requirements. The mesh of each zone was generated separately and then the mesh of the entire joint was produced by merging the meshes of all the sub-zones. This scheme can feasibly control the

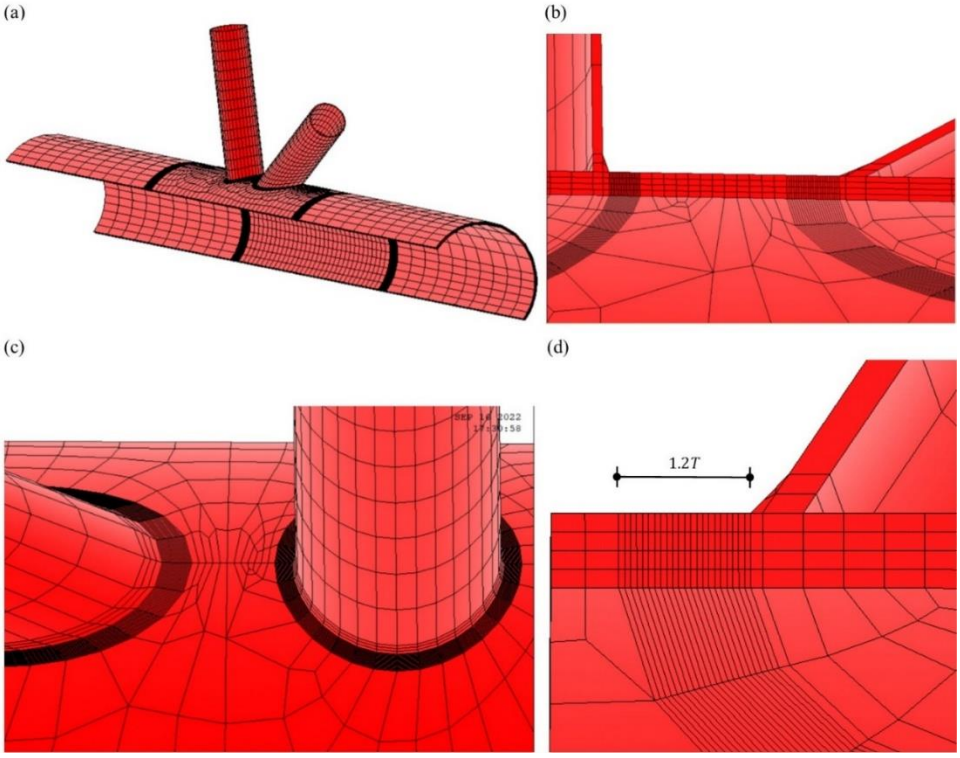

Fig. 6 Generated mesh by the sub-zone scheme

mesh quantity and quality and avoid badly distorted elements. The mesh generated by this procedure for a two-planar tubular DYT-joint is shown in Fig. 6(a).

It is explained in Sect. 3.4 that the geometric stresses perpendicular to the weld toe are required to be calculated in order to determine the DoB at the weld toe position based on Eq. (1). As shown in Fig. 6, to extract the geometric stresses perpendicular to the weld toe, the region near the weld toe was meshed finely. The width of this region is discussed in Sect. 3.4.

In order to make sure that the results of the FE analysis are not affected by the inadequate quality or the size of the generated mesh, convergence test was conducted and meshes with different densities were used in this test, before generating the 243 models. Based on the results of convergence test, the number of elements through the thickness of the chord was 7, 5, and 4 for the γ values of 12, 18, and 24, respectively; and the number of elements through the thickness of the brace member was 1 (Fig. 6(b)). The number of elements along a full brace-to-chord intersection was selected to be 32 for both the orthogonal and inclined braces (Fig. 6(c)). The number of elements on the surface, base, and back of the weld profile was 3, 1, and 2, respectively (Figs. 6(b) and 6(d)), and the number of elements inside the extrapolation region was 22 (Fig. 6(d)).

3.4 Analysis procedure and extraction of DoB values

In order to determine the DoB values in a tubular joint, static analysis of the linearly elastic type is suitable. The Young's modulus and Poisson's ratio were taken to be 207 GPa and 0.3, respectively.

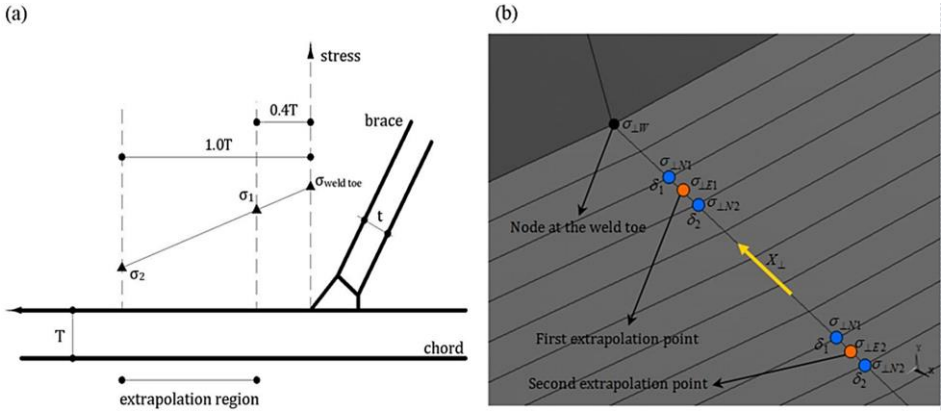

Fig. 7 (a) Extrapolation method according to IIW-2259-15 (2016) and (b) Required interpolations and extrapolations to extract the HSS value at the weld toe

In order to determine the weld-toe DoB values, according to Eq. (1), bending and membrane stress components should be known. These components can be calculated as follows

$$\sigma_B = \frac{\sigma_O - \sigma_I}{2} \tag{3}$$

$$\sigma_M = \frac{\sigma_O + \sigma_I}{2} \tag{4}$$

where σ_O and σ_I are the hot-spot stresses (HSSs) at the weld toe on the outer and inner surfaces of the chord, respectively.

Eqs. (2)-(4) lead to the following relation for the DoB based on the HSSs

$$\text{DoB} = \frac{1}{2}\left(1 - \frac{\sigma_I}{\sigma_O}\right) \tag{5}$$

To determine the HSSs, the stress at the weld-toe position should be extracted from the stress field outside the region influenced by the local weld-toe geometry. The location from which the stresses have to be extrapolated, called extrapolation region, depends on the dimensions of the joint and on the position along the intersection. According to the recommendations of International Institute of Welding IIW-2259-15 (2016), the first extrapolation point should be at a distance of $0.4T$ from the weld toe, and the second point must be $0.6T$ further from the first point (Fig. 7(a)). The HSS is obtained by the linear extrapolation of the geometric stresses at these two points to the weld toe.

To extract and extrapolate the stresses perpendicular to the weld toe, the region between the weld toe and the second extrapolation point was meshed in such a way that each extrapolation point was placed between two nodes located in its immediate vicinity. These nodes are located on the element-generated lines which are perpendicular to the weld toe (X_1 direction in Fig. 7(b)).

At an arbitrary node inside the extrapolation region, the stress component in the direction perpendicular to the weld toe can be calculated, through the transformation of primary stresses in the global coordinate system, using the following equation

$$\sigma_{\perp N} = \sigma_x l_1^2 + \sigma_y m_1^2 + \sigma_z n_1^2 + 2\left(\tau_{xy} l_1 m_1 + \tau_{yz} m_1 n_1 + \tau_{zx} n_1 l_1\right) \quad (6)$$

where σ_a and τ_{ab} (a, b = x, y, z) are components of the stress tensor which can be extracted from ANSYS analysis results; and l_1, m_1, and n_1 are transformation components.

At the saddle, crown, toe, and heel positions, Eq. (6) is simplified as

$$\sigma_{\perp N} = \sigma_y m_1^2 + \sigma_z n_1^2 + 2\tau_{yz} m_1 n_1 \quad \text{(Saddle)} \quad ; \quad \sigma_{\perp N} = \sigma_x \quad \text{(Crown, Toe, and Heel)} \quad (7)$$

Transformation components can be obtained as follows

$$m_1 = \cos\left(X_\perp, y\right) = \left(y_w - y_n\right)/\delta \quad ; \quad n_1 = \cos\left(X_\perp, z\right) = \left(z_w - z_n\right)/\delta \quad (8)$$

$$\delta = \sqrt{\left(x_w - x_n\right)^2 + \left(y_w - y_n\right)^2 + \left(z_w - z_n\right)^2} \quad (9)$$

where $X_\perp$ is the direction perpendicular to the weld toe (Fig. 7(b)); x, y, and z are the axes of global Cartesian coordinate system; (x_n, y_n, z_n) and (x_w, y_w, z_w) are coordinates of the considered node inside the extrapolation region and its corresponding node at the weld toe position, respectively; and δ is the distance between the weld toe and the considered node inside the extrapolation region.

The stress at an extrapolation point is obtained as follows

$$\sigma_{\perp E} = \frac{\sigma_{\perp N1} - \sigma_{\perp N2}}{\delta_1 - \delta_2}\left(\Delta - \delta_2\right) + \sigma_{\perp N2} \quad (10)$$

where $\sigma_{\perp Ni}$ (i = 1 and 2) is the nodal stress in the immediate vicinity of the extrapolation point in a direction perpendicular to the weld toe (Eq. (7)); δ_i (i = 1 and 2) is obtained by Eq. (9); and Δ equals to 0.4T and 1.0T for the first and second extrapolation points, respectively (Fig. 7(b)).

The extrapolated stress at the weld toe position, HSS, is calculated by the following equation:

$$\sigma_{\perp W} = \frac{1}{0.6}\sigma_{\perp E1} - \frac{0.4}{0.6}\sigma_{\perp E2} \quad (11)$$

where $\sigma_{\perp E1}$ and $\sigma_{\perp E2}$ are the stresses at the first and second extrapolation points in the direction perpendicular to the weld toe, respectively (Eq. (10)).

If the considered nodes in the calculations of Eqs. (7)-(11) are located on the outer surface of the chord, the value of $\sigma_{\perp W}$ obtained from Eq. (11) is used as σ_O in Eq. (5); and if the considered nodes are located on the inner surface of the chord, the result of Eq. (11) is equivalent to σ_I which is required for the calculation of the DoB in Eq. (5).

To facilitate the calculation of DoB values, above formulation was implemented in a macro file developed by the ANSYS parametric design language (APDL). The input data required to be provided by the user of the macro file are the chord thickness, label number of the node located at the weld toe, and the label numbers of the nodes inside the extrapolation region. These nodes can be introduced using the graphic user interface (GUI).

3.5 FE model verification

As far as the authors are aware, there is no experimental/numerical data available in the literature on the DoB values in two-planar tubular DYT-joints. However, a set of parametric equations have

Table 1 Geometrical properties of uniplanar tubular T-joint used for the verification of FE models

Parameter	D (mm)	T (mm)	L (mm)	d (mm)	t (mm)	l (mm)	τ	β	γ	α	α_B
Value	500	12.5	2500	300	6.25	1200	0.5	0.6	20	10	8

Table 2 Geometrical properties of uniplanar tubular K-joint used for the verification of FE models

Parameter	D (mm)	T (mm)	L (mm)	d (mm)	t (mm)	l (mm)	τ	β	γ	α	ζ	θ
Value	508	12.512	3200.40	254	12.512	1016	1.0	0.5	20.3	12.6	0.15	45°

Table 3 Results of the FE model verification based on available parametric equations

Position	DoB		Difference
	Present FE model	Chang and Dover (1999b) Eqs.	
Saddle	0.727	0.858 (Eq. (A7) of Chang and Dover (1999b))	15.24%
Crown	0.452	0.546 (Eq. (A8) of Chang and Dover (1999b))	17.21%

Table 4 Results of the FE model verification based on available parametric equations

Position	DoB		Difference
	Present FE model	Morgan and Lee (1998b) Eqs.	
Saddle	0.8288	0.9283 (Eq. (3(d)) of Morgan and Lee (1998b))	12.00%
Toe	0.8894	0.8989 (Eq. (3(f)) of Morgan and Lee (1998b))	1.06%
Heel	0.7502	0.6997 (Eq. (3(b)) of Morgan and Lee (1998b))	7.21%

been proposed by Chang and Dover (1999b) and Morgan and Lee (1998b) for the prediction of DoB values in axially loaded tubular T- and K-joints, respectively. These equations were used in the present study to validate the generated FE models. In order to so, two FE models were generated for T- and K-joints having typical geometrical characteristics (Tables 1 and 2) and the models were analyzed subjected to axial loading. Geometrical properties given in Tables 1 and 2 have been previously employed by Ahmadi *et al*. (2020) and Ahmadi and Alizadeh Atalo (2021) for FE model verification. The method of geometrical modeling (introducing the chord, orthogonal braces, inclined braces, and weld profiles), the mesh generation procedure (including the selection of element type and size), analysis method, and the method of DoB extraction are identical for the validating models and the joint models used for the parametric study. Hence, the verification of DoB values derived from validating FE models with the results of Chang and Dover (1999b) and Morgan and Lee (1998b) equations lends some support to the validity of DoB values derived from the two-planar joint FE models. Results of verification process presented in Tables 3 and 4 indicate that there is a good agreement between the results of present FE model and equations proposed by Chang and Dover (1999b) and Morgan and Lee (1998b); and the average difference is 10.5%. Hence, generated FE models can be considered to be accurate enough to provide valid results.

Table 5 Values assigned to each dimensionless parameter

Parameter	Definition	Value(s)
β	d/D	0.3, 0.4, 0.5
γ	$D/2T$	12, 18, 24
τ	t/T	0.4, 0.7, 1.0
α	$2L/D$	8, 16, 24
θ	Brace inclination angle	30°, 45°, 60°
ζ	g/D	0.2
α_B	$2l/d$	8

4. Geometrical effects on the DoB values

4.1 Settings of parametric study

To study the DoB in two-planar tubular DYT-joints subjected to axial loading (Fig. 1(c)), 243 models were generated and analyzed using the FE-based software, ANSYS. The objective was to investigate the effects of dimensionless geometrical parameters on the DoB values at the inner saddle, outer saddle, crown, toe, and heel positions.

Different values assigned to parameters β, γ, τ, θ, and α have been presented in Table 5. These values cover the practical ranges of dimensionless parameters typically found in tubular joints of offshore jacket structures. Providing that the gap between the braces is not very large, the relative gap ($\zeta = g/D$) has no considerable effect on the stress and strain distribution. The validity range for this statement is $0.2 \le \zeta \le 0.6$ (Lotfollahi-Yaghin and Ahmadi 2010). Hence, a typical value of $\zeta = 0.2$ was designated for all joints. The brace length has no effect on the HSS values when the parameter α_B is greater than a critical value (Chang and Dover 1999b). According to Chang and Dover (1996), this critical value is about 6. In the present study, in order to avoid the effect of short brace length, a realistic value of $\alpha_B = 8$ was assigned to all joints. The 243 generated models span the following ranges of dimensionless geometrical parameters

$$0.3 \le \beta \le 0.5 \; ; \; 12 \le \gamma \le 24 \; ; \; 0.4 \le \tau \le 1.0 \; ; \; 8 \le \alpha \le 24 \; ; \; 30^\circ \le \theta \le 60^\circ \qquad (12)$$

4.2 Effects of the β, τ, γ, θ, and α

The parameter β is the ratio of brace diameter to chord diameter. Hence, the increase of the β in models having constant value of chord diameter results in the increase of brace diameter. Six charts are given in Fig. 8, as an example, depicting the change of the DoB values at the outer crown (OOC), inner crown (OIC), inner saddle (OIS), and outer saddle (OOS) positions, on the chord-side weld toe of the orthogonal brace, as well as the toe (IT) and inner saddle (IIS) positions, on the chord-side weld toe of the inclined brace, due to the change in the value of the β and the interaction of this parameter with the τ. The OOC, OIC, OIS, OOS, IT, and IIS positions are shown in Fig. 1(b). In this study, the influence of parameters γ, α, and θ over the effect of the β on the DoB was also investigated.

A large number of comparative charts were used to study the effect of the β and only six of them are presented here for the sake of brevity. Results showed that the increase of the β generally results

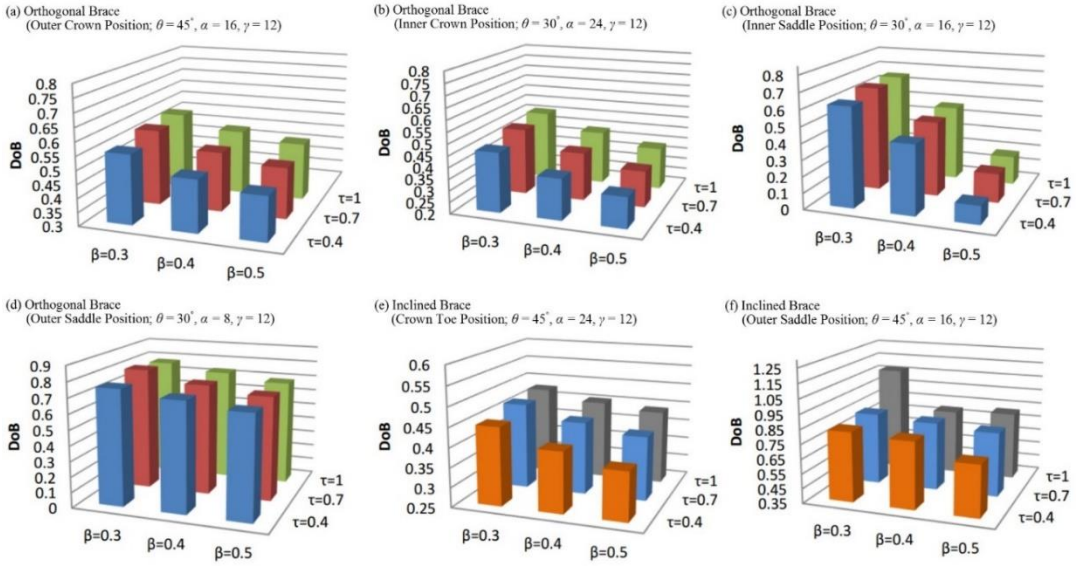

Fig. 8 The effect of the β on the DoB values and its interaction with the τ

in the decrease of the DoB values at all the considered positions. This conclusion is not dependent on values of other geometrical parameters.

The parameter τ is the ratio of brace thickness to chord thickness and the γ is the ratio of radius to thickness of the chord. Hence, the increase of the τ in models having constant value of the γ results in the increase of the brace thickness. For example, Fig. 9 shows the change of the DoB values at the OOC, OIC, OIS, OOS, IT, and IIS positions due to the change in the value of the τ and the interaction of this parameter with the θ. In this study, the interaction of the τ with the other geometrical parameters was also investigated. Results indicated that the increase of the τ leads to the increase of the DoB at studied positions of the orthogonal braces; while its increase results in the decrease of the DoB at the considered positions of the inclined brace. However, the amount of the DoB changes due to the increase of the τ is relatively small.

The parameter γ is the ratio of the radius to the thickness of the chord. Hence, the increase of the γ in models having constant value of the chord diameter means the decrease of chord thickness. Six charts are presented in Fig. 10, as an example, depicting the change of the DoB at the OOC, OIC, OIS, OOS, IT, and IIS positions due to the change in the value of the γ and the interaction of this parameter with the β. In this study, the influence of parameters τ, α, and θ over the effect of the γ on DoB values was also investigated. It was observed that the increase of the γ leads to the increase of the DoB at the inner and outer saddle positions; while its increase results in the decrease of the DoB at the crown and toe positions.

The parameter α is the ratio of the length to the radius of the chord. Hence, the increase of the α in models having constant value of the chord diameter means the increase of the chord length. For example, Fig. 11 shows the change of the DoB values the OOC, OIC, OIS, OOS, IT, and IIS positions due to the change in the value of the α and the interaction of this parameter with the β. In this study, the interaction of the α with the other geometrical parameters was also investigated. Results showed that the increase of the α generally leads to the decrease of the DoB at the crown and toe position; but it does not have a considerable effect on the DoB values at the saddle positions.

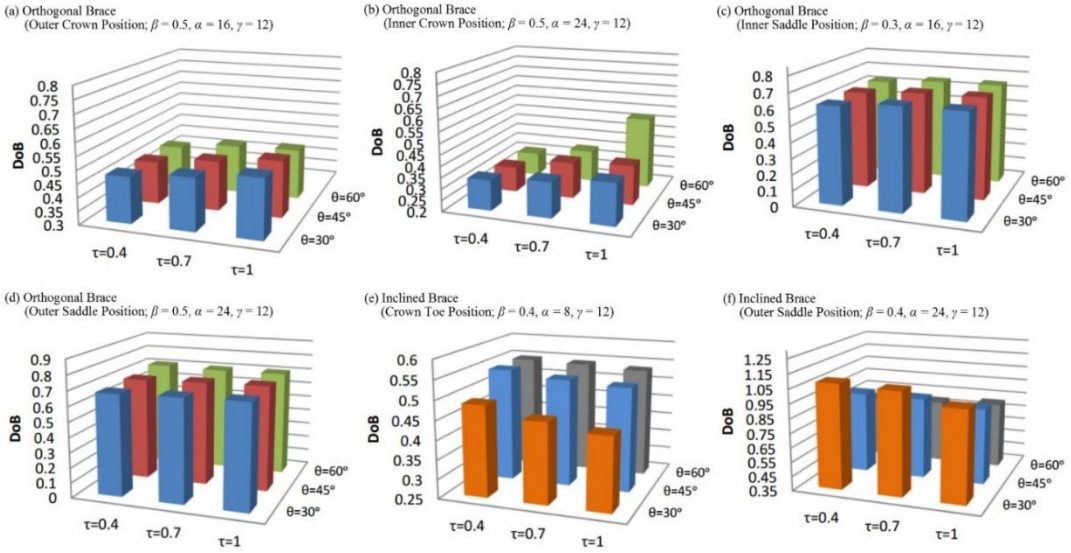

Fig. 9 The effect of the τ on the DoB values and its interaction with the θ

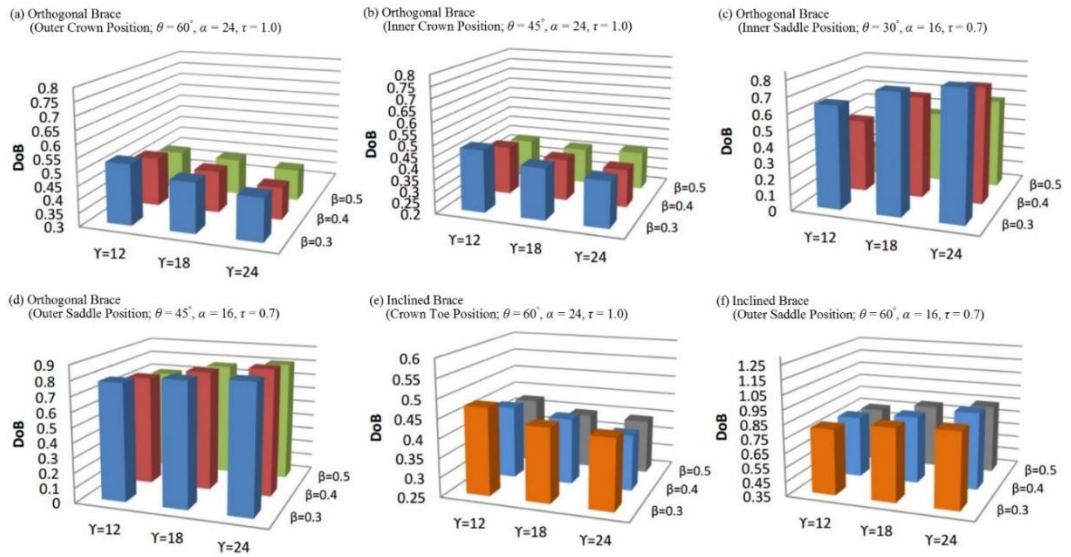

Fig. 10 The effect of the γ on the DoB values and its interaction with the β

The parameter θ is the brace inclination angle shown in Fig. 1(b). Six charts are presented in Fig. 12, as an example, depicting the change of the DoB at the OOC, OIC, OIS, OOS, IT, and IIS positions due to the change in the value of the θ and the interaction of this parameter with the β. In this study, the influence of parameters τ, γ, and α over the effect of the θ on DoB values was also investigated. It was observed that the increase of the θ does not have a considerable effect on the DoB values of the orthogonal brace. However, when the θ increases, the DoB at the toe position of the inclined brace increases; while the DoB value at the outer saddle position of the inclined brace decreases.

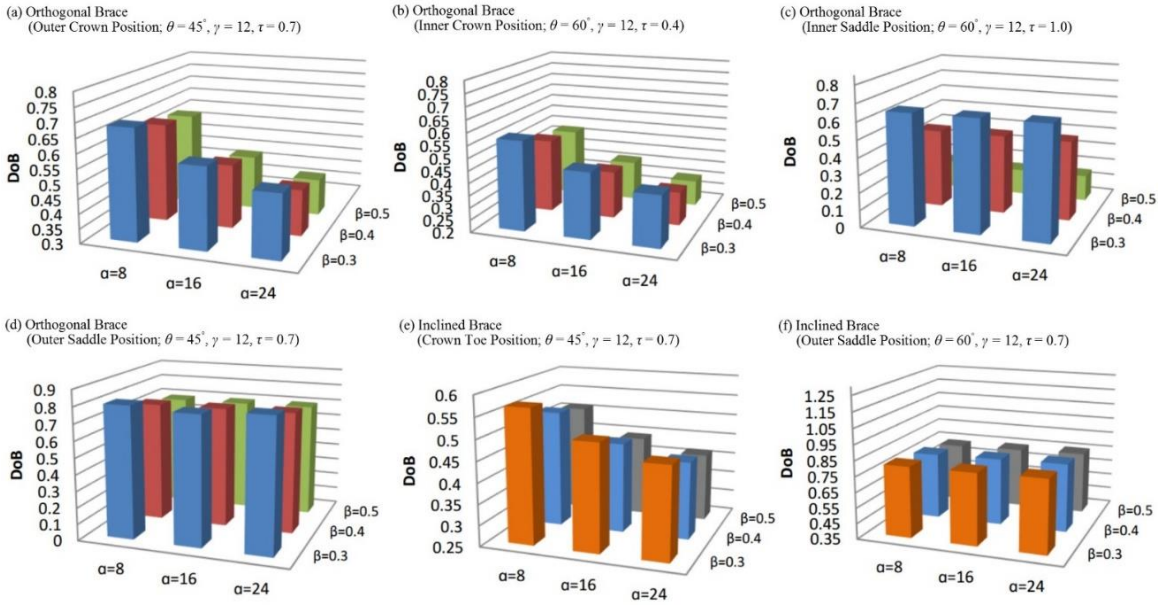

Fig. 11 The effect of the α on the DoB values and its interaction with the β

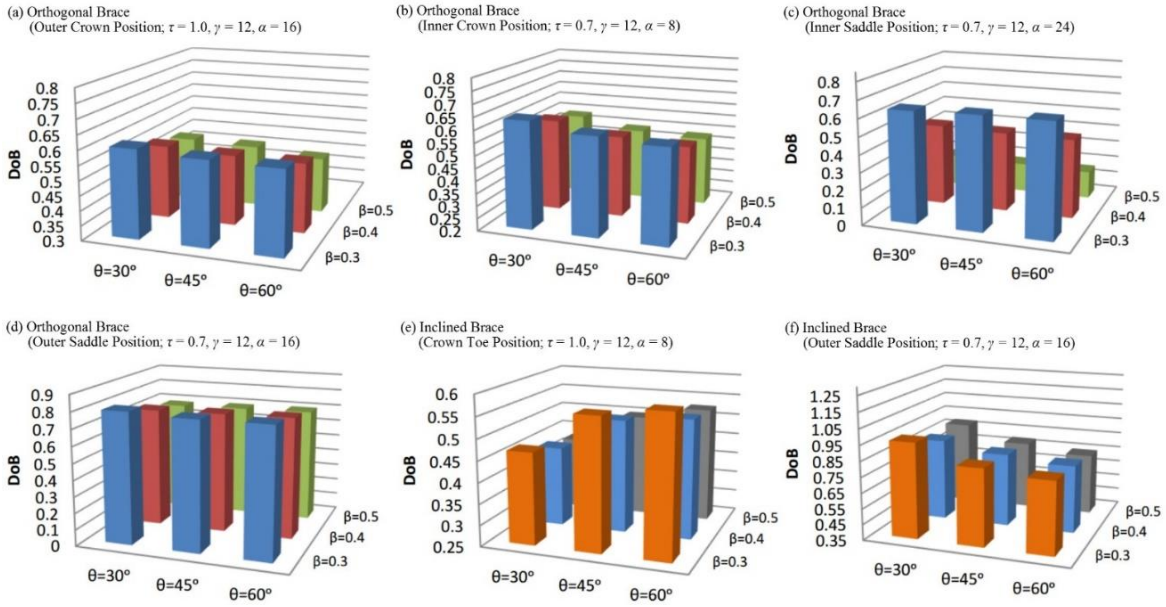

Fig. 12 The effect of the θ on the DoB values and its interaction with the β

It should be noted that the values of the DoB at the crown heel position of the inclined brace are not included in Figs. 8-12. The reason is that the SCF values at this position are always quite low (Table 6). Hence, the maximum HSS never occurs at this position and consequently the stress range at the crown heel position is never going to be used for the fatigue analysis in either the S-N or FM approaches. Therefore, the calculation of DoB at this position is not practically useful.

Table 6 Comparison of SCF values at different positions in nine sample two-planar DYT-joints subject to axial loading

Joint ID	Geometrical properties								SCF			
	D (mm)	τ	β	γ	ζ	θ	α	α_B	Inner saddle	Outer saddle	Toe	Heel
DYT9	500	0.4	0.3	12	0.2	60°	8	8	2.3092	3.4566	1.7555	0.8653
DYT10	500	0.4	0.3	18	0.2	30°	24	8	1.0578	2.3126	2.9166	0.9356
DYT11	500	0.4	0.3	18	0.2	30°	16	8	1.1292	2.3121	2.2757	0.3992
DYT12	500	0.4	0.3	18	0.2	30°	8	8	1.1777	2.4362	1.6813	0.1574
DYT13	500	0.4	0.3	18	0.2	45°	24	8	3.2591	5.6105	3.0309	1.7366
DYT14	500	0.4	0.3	18	0.2	45°	16	8	3.5509	5.8859	2.4596	1.2123
DYT15	500	0.4	0.3	18	0.2	45°	8	8	3.8351	6.1511	1.8967	0.6981
DYT16	500	0.4	0.3	18	0.2	60°	24	8	3.5056	5.5975	2.9266	2.1901
DYT17	500	0.4	0.3	18	0.2	60°	16	8	3.4764	5.6168	2.3660	1.6553

4.3 Remarks on low DoB

Figs. 8-12 indicate that DoB values smaller than 0.8 have been frequently observed in axially loaded two-planar YT-joints. The average DoB values for the 243 studied joint models at the outer crown, inner crown, inner saddle, and outer saddle, positions of the orthogonal braces are 0.5205, 0.4384, 0.5725, and 0.7886, respectively. For the inclined brace, the average DoB values are 0.4579 and 0.8578 at the toe and outer saddle positions, respectively. As mentioned earlier, typical DoB values are in the range of 0.8–0.9 for the joints used to derive the S-N curves; and smaller values can be considered as low DoB (Chang and Dover 1999b). Hence, it is quite common for an axially loaded two-planar YT-joint to have a low DoB. As previously discussed, Eide *et al*. (1993) has confirmed the detrimental effect of low DoB on fatigue life. Therefore, when the current standard HSS-based S-N approach is used for the fatigue analysis of axially loaded two-planar YT-joints, results should be modified to include the effect of the DoB in order to obtain more accurate fatigue life prediction.

4.4 Effect of multi-planarity on the DoB values

Fig. 13 compares the DoB values in three sample uniplanar and two-planar tubular YT-joints. Uniplanar YT-joints are also called N-joints. Geometrical properties of sample joints are given in Table 7. Fig. 13 indicates that there can be a quite big difference among the DoB values in uniplanar and two-planar YT-joints. For example, the DoB value at the inner crown position of the orthogonal brace in the two-planar DYT3 model is nearly three times the DoB at the crown position of the orthogonal brace in the corresponding uniplanar YT3 model (Fig. 13(b)); and the DoB value at the inner saddle position of the orthogonal brace in the two-planar DYT1 model is approximately 20% of the DoB at the saddle position of the orthogonal brace in the corresponding uniplanar YT1 model (Fig. 13(c)). Hence, it can be concluded that for axially loaded two-planar YT-joints, the parametric formulas of uniplanar YT-joints are not applicable for the DoB prediction, since such formulas may lead to under-/over-predicting results. Consequently, developing a set of specific parametric equations for the DoB calculation in two-planar YT-joints has practical value.

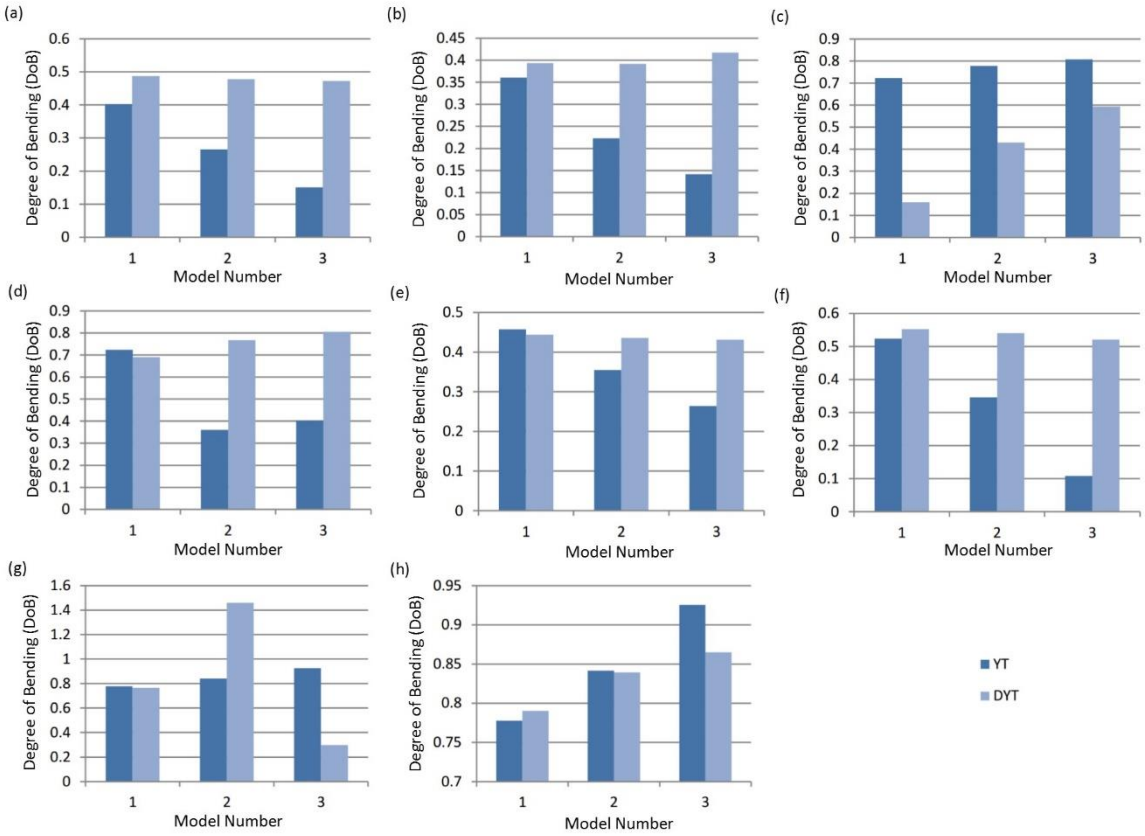

Fig. 13 Comparison of DoB values in six sample uniplanar YT- and two-planar DYT-joints (Table 7): (a) Outer crown position of the orthogonal brace, (b) Inner crown position of the orthogonal brace, (c) Inner saddle position of the orthogonal brace, (d) Outer saddle position of the orthogonal brace, (e) Toe position of the inclined brace, (f) Heel position of the inclined brace, (g) Inner saddle position of the inclined brace and (h) Outer saddle position of the inclined brace

Table 7 Geometrical properties of six sample joints used to compare the DoB values in uniplanar YT- and two-planar DYT-joints

Joint ID	Geometrical properties							
	D (mm)	τ	β	γ	ζ	θ	α	α_B
YT1 and DYT1	500	0.7	0.5	12	0.2	45°	16	8
YT2 and DYT2	500	0.7	0.5	18	0.2	45°	16	8
YT3 and DYT3	500	0.7	0.5	24	0.2	45°	16	8

5. Deriving parametric equations for the DoB calculation

Six individual parametric equations are proposed in the present paper, to calculate the DoB values at the inner saddle, outer saddle, inner crown, outer crown, and toe positions on the weld toe of two-

planar tubular DYT-joints subjected to axial loading. Results of multiple nonlinear regression analyses performed by SPSS were used to develop these parametric DoB formulas. Values of dependent variable (i.e., DoB) and independent variables (i.e., β, γ, τ, θ, and α) constitute the input data imported in the form of a matrix. Each row of this matrix involves the information about the DoB value at a considered position on the chord-side weld toe of a two-planar tubular DYT-joint having specific geometrical properties.

When the dependent and independent variables are defined, a model expression must be built with defined parameters. Parameters of the model expression are unknown coefficients and exponents. The researcher must specify a starting value for each parameter, preferably as close as possible to the expected final solution. Poor starting values can result in failure to converge or in convergence on a solution that is local (rather than global) or is physically impossible. Various model expressions must be built to derive a parametric equation having a high coefficient of determination (R^2).

Following parametric equations are proposed, after performing a large number of nonlinear analyses, for the calculation of DoB values at the inner saddle, outer saddle, inner crown, outer crown, and toe positions in tubular DYT-joints subjected to axial loading condition (Fig. 1(c)):

ORTHOGONAL BRACES:

- ***Outer crown position***

$$(\mathrm{DoB_{OC}})_{\mathrm{OB}} = -0.590\gamma^{-0.409}\beta^{0.745}\tau^{-0.003}\alpha^{-0.987}\left(1 + 136.692\alpha - 18.282\beta\alpha - \frac{14.735}{\gamma^{14.675}\tau^{6.923}\alpha^{5.886}}\right) + \frac{73.777}{\gamma^{0.399}\beta^{-0.655}} \qquad R^2 = 0.947 \qquad (13)$$

- ***Inner crown position***

$$(\mathrm{DoB_{IC}})_{\mathrm{OB}} = -2.277\gamma^{-0.590}\beta^{0.915}\tau^{-0.003}\alpha^{-0.992}\left(1 + 100.482\alpha - 12.105\beta\alpha - \frac{15.605}{\gamma^{14.070}\tau^{24.341}\alpha^{6.875}}\right) + \frac{206.896}{\gamma^{0.580}\beta^{-0.839}} \qquad R^2 = 0.871 \qquad (14)$$

- ***Inner saddle position***

$$(\mathrm{DoB_{IS}})_{\mathrm{OB}} = -3.890\gamma^{-0.099}\beta^{0.609}\tau^{0.058}\alpha^{0.009}(1 - 2.319\beta + 0.040\gamma\beta) \qquad R^2 = 0.979 \qquad (15)$$

- ***Outer saddle position***

$$(\mathrm{DoB_{OS}})_{\mathrm{OB}} = -0.007\gamma^{0.339}\beta^{-1.418}\tau^{0.033}\alpha^{0.005}(1 + 0.120\gamma - 38.668\beta - 0.039\gamma\beta + \tau^{0.992}\beta^{4.346}\alpha^{0.353}) \qquad R^2 = 0.971 \qquad (16)$$

INCLINED BRACES:

- ***Toe position***

$$(\mathrm{DoB_{T}})_{\mathrm{IB}} = 0.010\gamma^{0.815}\beta^{-0.132}\tau^{-0.584}\alpha^{0.060}\theta^{0.500}\left[1 - 1.576\theta - 0.021\beta\alpha + \left(\frac{68.896}{\gamma^{0.784}}\right)\tau^{0.407}\alpha^{-0.310}\right] + \frac{0.044}{\alpha^{-0.403}}\tau^{0.539} \qquad R^2 = 0.802 \qquad (17)$$

- ***Outer saddle position***

$$(\mathrm{DoB_{OS}})_{\mathrm{IB}} = -0.012\gamma^{-1.319}\beta^{-6.299}\tau^{0.079}\alpha^{-0.674}\theta^{-0.530}(1 + \tau^{-0.562}\beta^{7.964}\alpha^{3.009})(10.717\beta\cos\theta\sin^{3.811}\theta - 1.028\beta\tau^{0.107}\gamma^{0.348}) - 16.107\tau^{-0.002}\theta^{-0.007} + 10.767\beta^{-0.007}\arctan(\gamma\alpha) \qquad R^2 = 0.793 \qquad (18)$$

The value of θ is Eqs. (13)-(18) should be inserted in radians. Values obtained for R^2, indicating the accuracy of the fit, are considered to be acceptable regarding the complex nature of the problem.

The validity ranges of dimensionless geometrical parameters for the developed equations have been given in Eq. (12). It should be noted that, no design equation was developed for the heel position. The reason has been discussed in Sect. 4.2.

In Fig. 14, the DoB values predicted by proposed equations are compared with the DoB values extracted from FE analyses. It can be seen that there is a good agreement between the results of proposed equations and numerically computed values.

The UK Department of Energy (1983) recommends the following assessment criteria regarding the applicability of the parametric equations (P/R stands for the ratio of the *predicted* DoB from a given equation to the *recorded* DoB from test or analysis):

- For a given dataset, if % DoB values under-predicting $\leq$ 25%, i.e., [%P/R < 1.0] $\leq$ 25%, and if % SCFs considerably under-predicting $\leq$ 5%, i.e., [%P/R < 0.8] $\leq$ 5%, then accept the equation. If, in addition, the percentage DoB values considerably over-predicting $\leq$ 50%, i.e., [%P/R > 1.5] $\geq$50%, then the equation is regarded as generally conservative.
- If the acceptance criteria is nearly met i.e., 25% < [%P/R < 1.0] $\leq$ 30%, and/or 5% < [%P/R < 0.8] $\leq$ 7.5%, then the equation is regarded as borderline and engineering judgment must be used to determine acceptance or rejection.
- Otherwise reject the equation as it is too optimistic.

In view of the fact that for a mean fit equation, there is always a large percentage of under-prediction, the requirement for joint under-prediction, i.e., P/R < 1.0, can be completely removed in the assessment of parametric equations (Bomel Consulting Engineers 1994). Assessment results are presented in Table 8 showing that Eqs. (13)-(18) satisfy the UK DoE criteria in their present form, and hence can reliably be used for the analysis and design of tubular DYT-joints commonly found in offshore jacket structures.

Table 8 Results of DoB equations assessment according to the UK DoE (1983) acceptance criteria

Proposed equation	Conditions		Decision
	%P/R < 0.8	%P/R > 1.5	
Eq. (13)	0.00% < 5% OK.	0.00% < 50% OK.	Accept
Eq. (14)	0.41% < 5% OK.	0.00% < 50% OK.	Accept
Eq. (15)	0.00% < 5% OK.	3.29% < 50% OK.	Accept
Eq. (16)	0.00% < 5% OK.	0.00% < 50% OK.	Accept
Eq. (17)	0.00% < 5% OK.	0.00% < 50% OK.	Accept
Eq. (18)	0.00% < 5 % OK.	0.00% < 50% OK.	Accept

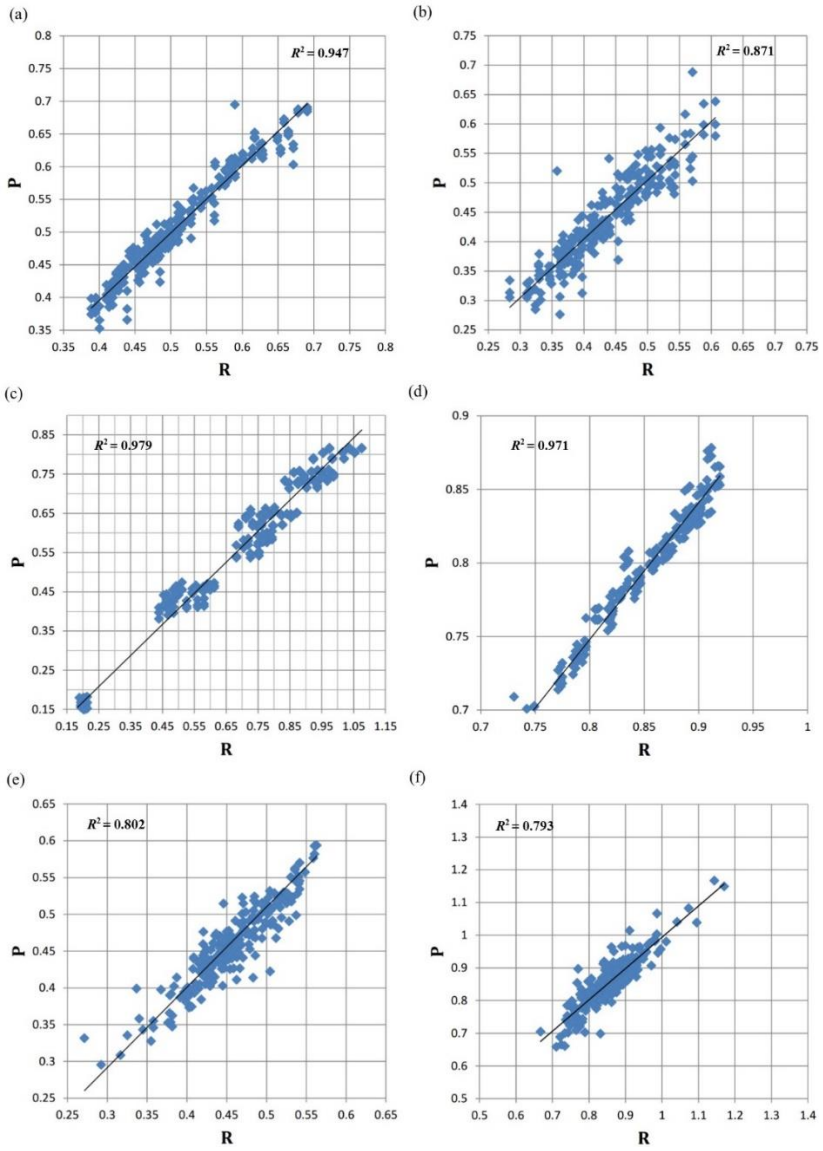

Fig. 14 Comparison of 243 DoB values calculated by the proposed equations with the corresponding DoB values extracted from the FE analysis (P: DoB value predicted by the equation, R: DoB value recorded from FE analysis): (a) Outer crown position of the orthogonal brace (Eq. (13)), (b) Inner crown position of the orthogonal brace (Eq. (14)), (c) Inner saddle position of the orthogonal brace (Eq. (15)), (d) Outer saddle position of the orthogonal brace (Eq. (16)), (e) Toe position of the inclined brace (Eq. (17)) and (f) Outer saddle position of the inclined brace (Eq. (18))

6. Application of DoB to improve the accuracy of fatigue life estimation

As mentioned earlier, there are two main approaches for the fatigue life estimation: stress-life (S-N) approach and fracture mechanics (FM) approach.

In S-N approach, detrimental effect of low DoB on the fatigue life can be considered during the application of S-N curves. One option is to use the same modification format recommended by Sect. 5.5.2 of API RP 2A-WSD (2007) for considering the so-called thickness effect. i.e., if the joint's DoB is smaller than a critical value (e.g., 0.8), the number of stress cycles leading to the joint failure (N_0), which has been obtained from a standard S-N curve, should be modified as follows

$$N = N_0 \left(\frac{\text{DoB}}{\text{DoB}_0} \right)^{\alpha} \tag{19}$$

where N is the modified number of stress cycles leading to the joint failure, DoB is the joint's degree of bending calculated by proposed equations (Eqs. (13)-(18)), DoB_0 is the critical value (e.g., 0.8), and the power α is a function of the joint geometry and quality of the weld that should be determined experimentally.

Fatigue life assessment based on FM approach involves calculating the number of stress cycles required for a given increase in crack size. This is implemented by assuming a suitable crack growth law such as the Paris equation. Using this technique, the number of stress cycles required to extend a fatigue crack from an initial depth a_i to any depth a_f is given as (Paris and Erdogan 1963)

$$N = \int_{a_i}^{a_f} \left(\frac{1}{C(\Delta K)^m} \right) da \tag{20}$$

where C and m are material constants, and ΔK is the SIF range which expresses the effect of load range on the crack. It describes the stress field associated with the cracked body at the crack tip

$$\Delta K = K_{\max} - K_{\min} = Y(a)\Delta\sigma\sqrt{\pi a} \tag{21}$$

where $\Delta\sigma$ is the HSS range, a is the crack size, and Y is the modifying shape parameter that depends on the crack geometry and the geometry of the specimen.

The accurate determination of the SIF is the key for FM calculations. Owing to the complexities introduced by the structural geometry and the nature of the local stress fields, it is impossible to calculate the SIFs analytically. This problem is often tackled by using the simplified models, such as the flat plate solution (Newman and Raju 1986) and methods based on the T-Butt weight function (Chang 1997), with an appropriate load shedding model. The general equation for calculating T-butt K value is

$$K = \left[Mk_m M_m \sigma_m + Mk_b M_b \sigma_b \right] \sqrt{\pi a} \tag{22}$$

where a is the crack depth, Mk is the weld-toe magnification factor, M is the plain plate shape factor, σ is the nominal plate stress, and subscripts m and b denote membrane and bending loadings, respectively. To approximate the K value for a tubular joint using T-butt solutions, Eq. (22) may be rewritten as follows (Lee and Bowness 2002)

$$K_{\text{tubular joint}} = \left[Mk_m M_m \text{SCF}(1 - \text{DoB}) + Mk_b M_b \text{SCF}.(\text{DoB}) \right] \sigma_n \sqrt{\pi a} \tag{23}$$

where σ_n denotes the nominal stress.

Eq. (23) shows that the standard stress-life approach may be unconservative for the joints with low DoB values. The reason is that in FM method, despite the stress-life approach, lower DoB may lead to a higher K value and consequently a lower number of cycles to failure (Eq. (20)).

7. Conclusions

Results of stress analyses performed on 243 FE models verified against available parametric equations were used to investigate the effects of geometrical parameters on the DoB values at the inner saddle, outer saddle, inner crown, outer crown, and toe positions on the weld toe of orthogonal and inclined braces in two-planar tubular DYT-joints under axial loading. A set of DoB parametric equations was also developed for the fatigue design. Main conclusions can be summarized as follows.

The increase of the β generally results in the decrease of the DoB values at all the considered positions. The increase of the τ leads to the increase of the DoB at studied positions of the orthogonal braces; while its increase results in the decrease of the DoB at the considered positions of the inclined brace. However, the amount of the DoB changes due to the increase of the τ is relatively small. The increase of the γ leads to the increase of the DoB at the inner and outer saddle positions; while its increase results in the decrease of the DoB at the inner crown, outer crown, and toe positions. The increase of the α generally leads to the decrease of the DoB at the inner crown, outer crown, and toe positions; but it does not have a considerable effect on the DoB values at the inner and outer saddle positions. The increase of the θ does not have a considerable effect on the DoB values of the orthogonal brace. However, when the θ increases, the DoB at the toe position of the inclined brace increases; while the DoB value at the outer saddle position of the inclined brace decreases.

DoB values smaller than 0.8 were frequently observed in axially loaded two-planar DYT-joints. Hence, it is quite common for a DYT-joint to have a low DoB subjected to axial loading. Detrimental effect of low DoB on fatigue life has been confirmed. Therefore, when the current standard HSS-based S-N approach is used for the fatigue analysis of axially loaded two-planar DYT-joints, results should be modified to include the effect of the DoB in order to obtain more accurate fatigue life prediction.

There can be a quite big difference between the DoB values in uniplanar YT- and two-planar DYT-joints. Hence, for axially loaded two-planar DYT-joints, the parametric formulas of uniplanar YT-joints are not applicable for the DoB prediction, since such formulas may lead to under-/over-predicting results. Consequently, developing a set of specific parametric equations for the DoB calculation in DYT-joints has practical value. Relatively high coefficients of determination and the satisfaction of acceptance criteria recommended by the UK DoE guarantee the accuracy of the six parametric equations proposed in the present paper. Hence, the developed equations can reliably be used for the fatigue analysis and design of two-planar tubular DYT-joints subjected to axial loading.

Acknowledgments

Useful comments of anonymous reviewers on draft version of this paper are highly appreciated.

References

Ahmadi, H. and Alizadeh Atalo, A. (2021), "Geometrical effects on the degree of bending (DoB) of multi-planar tubular KK-joints in jacket substructure of offshore wind turbines", *Appl. Ocean Res.*, **111**, 102678. https://doi.org/10.1016/j.apor.2021.102678.

Ahmadi, H. and Amini Niaki, M. (2019), "Effects of geometrical parameters on the degree of bending (DoB) in two-planar tubular DT-joints of offshore jacket structures subjected to axial and bending loads", *Mar.*

Struct., **64**, 229-245. https://doi.org/10.1016/j.marstruc.2018.11.008.
Ahmadi, H. and Asoodeh, S. (2016), "Parametric study of geometrical effects on the degree of bending (DoB) in offshore tubular K-joints under out-of-plane bending loads", *Appl. Ocean Res.*, **58**, 1-10. https://doi.org/10.1016/j.apor.2016.03.004.
Ahmadi, H., Chamani, S. and Kouhi, A. (2020), "Effects of geometrical parameters on the degree of bending (DoB) in multi-planar tubular XT-joints of offshore structures subjected to axial loading", *Appl. Ocean Res.*, **104**, 102381. https://doi.org/10.1016/j.apor.2020.102381.
Ahmadi, H. and Imani, H. (2022), "SCFs in offshore two-planar tubular TT-joints reinforced with internal ring stiffeners", *Ocean Syst. Eng.*, **12**(1), 1-22. https://doi.org/10.12989/ose.2022.12.1.001.
Ahmadi, H., Lotfollahi-Yaghin, M.A. and Asoodeh, S. (2015), "Degree of bending (DoB) in tubular K-joints of offshore structures subjected to in-plane bending (IPB) loads: Study of geometrical effects and parametric formulation", *Ocean Eng.*, **102**, 105-116. https://doi.org/10.1016/j.oceaneng.2015.04.050.
Ahmadi, H. and Zavvar, E. (2020), "Degree of bending (DoB) in offshore tubular KT-joints under the axial, in-plane bending (IPB), and out-of-plane bending (OPB) loads", *Appl. Ocean Res.*, **95**, 102015. https://doi.org/10.1016/j.apor.2019.102015.
American Petroleum Institute (2007), "Recommended practice for planning, designing and constructing fixed offshore platforms: Working stress design: RP 2A-WSD", 21st Ed., Errata and Supplement 3, Washington DC, US.
American Welding Society (2002), "Structural welding code: AWS D 1.1", Miami (FL), US.
Asgarian, B., Mokarram, V. and Alanjari, P. (2014), "Local joint flexibility equations for Y-T and K-type tubular joints", *Ocean Syst. Eng.*, **4**(2), 151-167. https://doi.org/10.12989/ose.2014.4.2.151.
Bao, S., Wang, W., Zhou, J., Qi, S. and Li, X. (2022), "Experimental study of hot spot stress for three-planar tubular Y-joint: I. Basic loads", *Thin-Wall. Struct.*, **177**, 109418. https://doi.org/10.1016/j.tws.2022.109418.
Bao, S., Wang, W., Li, X., Qi, S. and Zhou, J. (2022), "Experimental study of hot spot stress for three-planar tubular Y-joint: II. Combined loads", *Thin-Wall. Struct.*, **177**, 109416. https://doi.org/10.1016/j.tws.2022.109416.
Bao, S., Wang, W., Li, X. and Zhao, H. (2020), "Hot-spot stress caused by out-of-plane bending moments of three-planar tubular Y-joints", *Appl. Ocean Res.*, **100**, 102179. https://doi.org/10.1016/j.apor.2020.102179.
Bao, S., Wang, W., Zhou, J. and Li, X. (2023), "Study on hot spot stress distribution of three-planar tubular Y-joints subjected to in-plane bending moment", *Mar. Struct.*, **87**, 103326. https://doi.org/10.1016/j.marstruc.2022.103326.
Bomel Consulting Engineers (1994), "Assessment of SCF equations using Shell/KSEPL finite element data", C5970R02.01 REV C.
Chang, E. and Dover, W.D. (1999a), "Parametric equations to predict stress distributions along the intersection of tubular X and DT-joints", *Int. J. Fatigue*, **21**, 619-635. https://doi.org/10.1016/S0142-1123(99)00018-3.
Chang, E. and Dover, W.D. (1999b), "Prediction of degree of bending in tubular X and DT joints", *Int. J. Fatigue*, **21**, 147-161. https://doi.org/10.1016/S0142-1123(98)00060-7.
Chang, E., Dover, W.D. (1996), "Stress concentration factor parametric equations for tubular X and DT joints", *Int. J. Fatigue*, **18**, 363-387. https://doi.org/10.1016/0142-1123(96)00017-5.
Chang, E. (1997), "Parametric study of non-destructive fatigue strength evaluation of offshore tubular welded joints", PhD Thesis, University College London, UK.
Connolly, M.P.M. (1986), "A fracture mechanics approach to the fatigue assessment of tubular welded Y and K-joints", PhD Thesis, University College London, UK.
Det Norske Veritas (2005), "Fatigue design of offshore steel structures", Recommended Practice, DNV RP C203, Norway.
Det Norske Veritas (2008), "Structural design of offshore units (WSD method)", Offshore Standard, DNV OS C201, Norway.
Efthymiou, M. (1988), "Development of SCF formulae and generalized influence functions for use in fatigue analysis", OTJ 88, Surrey, UK.
Eide, O.I., Skallerud, B. and Berge, S. (1993), "Fatigue of large scale tubular joints–effects of sea water and spectrum loading", *Proceedings of the Fatigue under Spectrum Loading and in Corrosive Environments*

Conference, Technical University of Denmark, Lyngby, Denmark.
Hellier, A.K., Connolly, M. and Dover, W.D. (1990), "Stress concentration factors for tubular Y and T-joints", *Int. J. Fatigue*, **12**, 13-23. https://doi.org/10.1016/j.ijfatigue.2020.105719.
Hobbacher, A.F. (2016), "Recommendations for fatigue design of welded joints and components", IIW Document IIW-2259-15 ex XIII-2460-13/XV-1440-13, International Institute of Welding.
Ju, S.H. (2022), "Increasing the fatigue life of offshore wind turbine jacket structures using yaw stiffness and damping", *Renew. Sust. Energ. Rev.*, **162**, 112458. https://doi.org/10.1016/j.rser.2022.112458.
Lee, M.M.K. and Bowness, D. (2002), "Estimation of stress intensity factor solutions for weld toe cracks in offshore tubular joints", *Int. J. Fatigue*, **24**, 861-875. https://doi.org/10.1016/S0142-1123(01)00209-2.
Lie, S.T., Lee, C.K. and Wong, S.M. (2001), "Modeling and mesh generation of weld profile in tubular Y-joint", *J. Const. Steel Res.*, **57**, 547-567. https://doi.org/10.1016/S0143-974X(00)00031-6.
Lotfollahi-Yaghin, M.A. and Ahmadi, H. (2010), "Effect of geometrical parameters on SCF distribution along the weld toe of tubular KT-joints under balanced axial loads", *Int. J. Fatigue*, **32**, 703-719. https://doi.org/10.1016/j.ijfatigue.2009.10.008.
Morgan, M.R. and Lee, M.M.K. (1998a), "Parametric equations for distributions of stress concentration factors in tubular K-joints under out-of-plane moment loading", *Int. J. Fatigue*, **20**, 449-461. https://doi.org/10.1016/S0142-1123(98)00011-5.
Morgan, M.R. and Lee, M.M.K. (1998b), "Prediction of stress concentrations and degrees of bending in axially loaded tubular K-joints", *J. Const. Steel Res.*, **45**, 67-97. https://doi.org/10.1016/S0143-974X(97)00059-X.
Nassiraei, H. and Rezadoost, P. (2020), "Stress concentration factors in tubular T/Y-joints strengthened with FRP subjected to compressive load in offshore structures", *Int. J. Fatigue*, **140**, 105719. https://doi.org/10.1016/j.ijfatigue.2020.105719.
Nassiraei, H. and Rezadoost, P. (2021a), "Stress concentration factors in tubular T/Y-connections reinforced with FRP under in-plane bending load", *Mar. Struct.*, **76**, 102871, https://doi.org/10.1016/j.marstruc.2020.102871.
Nassiraei, H. and Rezadoost, P. (2021b), "Parametric study and formula for SCFs of FRP-strengthened CHS T/Y-joints under out-of-plane bending load", *Ocean Eng.*, **221**, 108313. https://doi.org/10.1016/j.oceaneng.2020.108313.
Nassiraei, H. and Rezadoost, P. (2021c), "Stress concentration factors in tubular X-connections retrofitted with FRP under compressive load", *Ocean Eng.*, **229**, 108562. https://doi.org/10.1016/j.oceaneng.2020.108562.
Nassiraei, H. and Rezadoost, P. (2021d), "SCFs in tubular X-connections retrofitted with FRP under in-plane bending load", *Compos. Struct.*, **274**, 114314. https://doi.org/10.1016/j.compstruct.2021.114314.
Nassiraei, H. and Rezadoost, P. (2021e), "SCFs in tubular X-joints retrofitted with FRP under out-of-plane bending moment", *Mar. Struct.*, **79**, 103010. https://doi.org/10.1016/j.marstruc.2021.103010.
Nassiraei, H. and Rezadoost, P. (2022a), "Stress concentration factors in tubular T-joints reinforced with external ring under in-plane bending moment", *Ocean Eng.*, **266**, 112551. https://doi.org/10.1016/j.oceaneng.2022.112551.
Nassiraei, H. and Rezadoost, P. (2022b), "Probabilistic analysis of the SCFs in tubular T/Y-joints reinforced with FRP under axial, in-plane bending, and out-of-plane bending loads", *Struct.*, **35**, 1078-1097. https://doi.org/10.1016/j.istruc.2021.06.029.
Nassiraei, H. and Rezadoost, P. (2022c), "Development of a probability distribution model for the SCFs in tubular X-connections retrofitted with FRP", *Struct.*, **36**, 233-247. https://doi.org/10.1016/j.istruc.2021.10.033.
Newman, J.C. and Raju, I.S. (1986), "Stress intensity factors equations for cracks in three dimensional finite bodies subjected to tension and bending loads", *Proceedings of the Conference on Computational Methods in the Mechanics of Fracture*, Amsterdam, Netherlands.
Paris, P. and Erdogan, F. (1963), "A critical analysis of crack propagation laws", *J. Basic Eng.*, **85**, 528-534. https://doi.org/10.1115/1.3656900.
Prashob, P.S., Shashikala, A.P. and Somasundaran, T.P. (2018), "Effect of FRP parameters in strengthening the tubular joint for offshore structures", *Ocean Syst. Eng.*, **8**(4), 409-426.

https://doi.org/10.12989/ose.2018.8.4.409.
Shao, Y.B., Du, Z.F. and Lie, S.T. (2009), "Prediction of hot spot stress distribution for tubular K-joints under basic loadings", *J. Const. Steel Res.*, **65**, 2011-2026. https://doi.org/10.1016/j.jcsr.2009.05.004.
Shao, Y.B. and Lie, S.T. (2005), "Parametric equation of stress intensity factor for tubular K-joint under balanced axial loads", *Int. J. Fatigue*, **27**, 666-679. https://doi.org/10.1016/j.ijfatigue.2004.11.003.
Shao, Y.B. (2006), "Analysis of stress intensity factor (SIF) for cracked tubular K-joints subjected to balanced axial load", *Eng. Fail. Anal.*, **13**, 44-64, https://doi.org/10.1016/j.engfailanal.2004.12.031.
Shao, Y.B. (2007), "Geometrical effect on the stress distribution along weld toe for tubular T- and K-joints under axial loading", *J. Const. Steel Res.*, **63**, 1351-1360. https://doi.org/10.1016/j.jcsr.2006.12.005.
Shen, W. and Choo, Y.S. (2012), "Stress intensity factor for a tubular T-joint with grouted chord", *Eng. Struct.*, **35**, 37-47. https://doi.org/10.1016/j.engstruct.2011.10.014.
Smedley, P. and Fisher, P. (1991), "Stress concentration factors for simple tubular joints", *Proceedings of the International Offshore and Polar Engineering Conference (ISOPE)*, Edinburgh.
Sunday, K. and Brennan, F. (2021), "A review of offshore wind monopiles structural design achievements and challenges", *Ocean Eng.*, **235**, 109409. https://doi.org/10.1016/j.oceaneng.2021.109409.
UK Department of Energy (1983), "Background notes to the fatigue guidance of offshore tubular joints", UK DoE, London, UK.
Wang, L., Kolios, A., Liu, X., Venetsanos, D. and Cai, R. (2022), "Reliability of offshore wind turbine support structures: A state-of-the-art review", *Renew. Sust. Energ. Rev.*, **161**, 112250. https://doi.org/10.1016/j.rser.2022.112250.

PS